83-690

26/XII-83

6785/83

E1-83-690

V.M.Bystritsky, V.P.Dzhelepov, A.Guła ,
V.A.Stolupin, J.Woźniak

DETERMINATION OF OPTIMAL CONDITIONS FOR THE EXPERIMENTAL INVESTIGATION OF MUON CATALYSIS OF NUCLEAR REACTION: $t+t-{}^{4}He+2n$

1983

1. INTRODUCTION

The discovery of a resonance character of the $dd\mu$-molecule formation[1,2] in the sequence of processes leading to nuclear reaction

$$d + d \to {}^3He + n \tag{1}$$

has given rise to a renewed interest in the investigation of the muon-catalysis of nuclear fusion processes. In subsequent experiments[3] the high formation rate has been established also for $dt\mu$-molecules, which has confirmed earlier theoretical predictions[4] of the presence of an analogous resonance mechanism in the muon catalysis of reaction

$$d + t \to {}^4He + n . \tag{2}$$

The latter result indicates that, apart from purely physical interest, further studies in this area deserve effort also in view of the emerging possibility of the practical application of the muon catalysis in energy production[5].

Extensive projects of investigation of the muon catalysis of nuclear fusion are now under way at several laboratories. The general idea of these projects is visualized in Fig.1 which presents the dominant processes leading to nuclear fusion in a deuterium-tritium mixture. The main interest lies undoubtedly in the investigation of the muon catalysis of reaction (2). It is seen, however, that the $dt\mu$-fusion is unavoidably accompanied by competitive processes leading to other nuclear reactions. In the first stage the most important of them are:

a) the chain of processes leading to reaction (1)

$$\mu + D_2 \to d\mu + D$$

$$\downarrow$$

$$d\mu + D_2 \xrightarrow[\text{formation}]{\text{resonant}} [(dd\mu)d2e]^* , \tag{3}$$

$$\downarrow$$

fusion

1

b) the chain
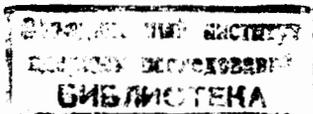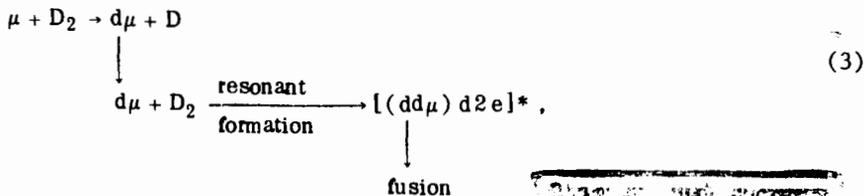
$$\mu + T_2 \rightarrow t\mu + T$$
$$\downarrow$$
$$t\mu + T_2 \longrightarrow [(tt\mu)te]^+ + e \qquad (4)$$
$$\downarrow$$
fusion

leading to nuclear fusion

$$t + t \longrightarrow {}^4He + 2n. \qquad (5)$$
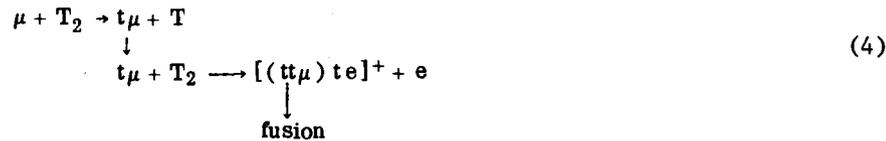
Chains (3) and (4) can be studied separately using pure deuterium and tritium targets. Such relatively simple experiments are necessary to obtain the required input information for the analysis of the full scheme of Fig.1.
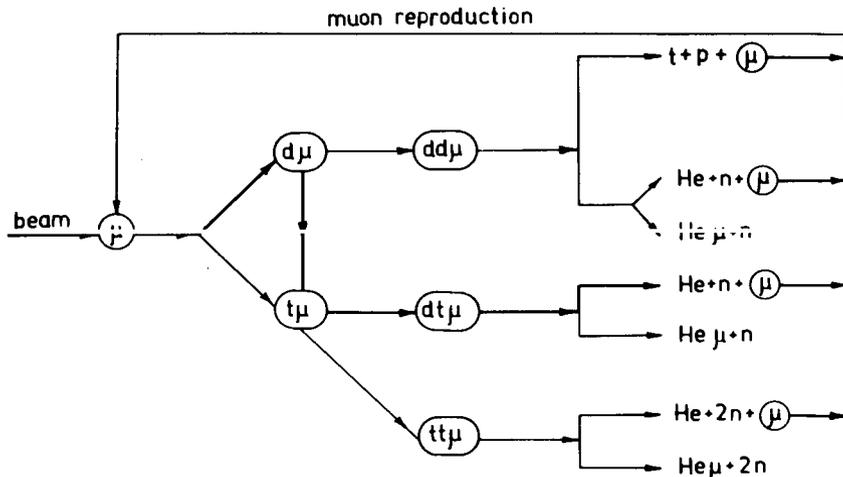
Fig.1. Dominant processes leading to nuclear fusion in a deuterium-tritium mixture.

Chain (3) has already been studied in several experiments[1,2,6]. The data agree reasonably well with the theoretical predictions, though some discrepancies between the results of Ref.[2] and Ref.[6] remain to be clarified. This notwithstanding, the obtained results confirm the presence of a resonance mechanism in the $dd\mu$-molecule formation (reflected in the temperature dependence of the corresponding formation rate) which can be explained by existence of a weakly bound state in the $dd\mu$-molecule.

On the other hand, no experimental data exist so far concerning chain (4). According to theoretical predictions[7] the $tt\mu$-molecule formation should proceed here via a nonresonant Auger-electron-ejection mechanism. Additionally, in contrast to reaction (1), where fusion rate in the $dd\mu$-molecule exceeds by several orders of magnitude the $dd\mu$-formation rate itself ($\sim 10^9 s^{-1}$ vs $\sim 10^5 \div 10^6 s^{-1}$), the two rates for reaction (5) may have comparable values[7,8]. This poses new problems for the experimental investigation of the $tt\mu$-fusion which are the subject of discussion in this paper.

In the next Section we present the formulae describing the kinetics of processes (4) and recall the definitions of appropriate parameters. The sensitivity of the experimental characteristics of chain (4) to the values of parameters is discussed in Section 3. Section 4 contains concluding remarks.

2. KINETIC FORMULAE AND DEFINITIONS OF PARAMETERS

The kinetics of processes (4) is described by the following set of coupled differential equations

$$\frac{dN_\mu}{dt} = -(\lambda_0 + \lambda_a) N_\mu + (1 - \omega) \lambda_f N_{tt\mu}, \qquad (6.1)$$

$$\frac{dN_{t\mu}}{dt} = -(\lambda_0 + \lambda_{tt\mu}) N_{t\mu} + \lambda_a N_\mu, \qquad (6.2)$$

$$\frac{dN_{tt\mu}}{dt} = -(\lambda_0 + \lambda_f) N_{tt\mu} + \lambda_{tt\mu} N_{t\mu}, \qquad (6.3)$$

$$\frac{dN_n}{dt} = 2\lambda_f N_{tt\mu}, \qquad (6.4)$$

where N_μ, $N_{t\mu}$, $N_{tt\mu}$ and N_n are the numbers of muons, $t\mu$-atoms, $tt\mu$-molecules and final neutrons, respectively. The kinetics given by Eqs. (6) does not include the mesomolecular processes involving ${}^3He$ produced in tritium β-decay (see the discussion in the next Section). The second term in the RHS of Eq. (6.1) reflects the reproduction of muons which are released free after fusion reaction (5) has taken place. Factor of two in Eq. (6.4) takes account of the two neutrons in the final state.

The parameters entering Eqs.(6) are: λ_0 - muon decay rate ($\lambda_0 = 0.455 \cdot 10^6 s^{-1}$), λ_a - formation rate of μ-atoms in the ground state, $\lambda_{tt\mu}$ - formation rate of the $tt\mu$-molecules, λ_f - fusion rate in the $tt\mu$-molecule, ω - probability of muon "sticking" to ${}^4He$ in the final state of reaction (5).

Determination of the parameters entering Eqs.(6) is most naturally based on the analysis of the final neutron time-distribution, dN_n/dt, which can be easily measured and involves all of the sought-for quantities. As the processes of $t\mu$ and $tt\mu$ -formation take place in collisions of muons ($t\mu$ -atoms) with tritium molecules, the corresponding rates can be assumed proportional to target density

$$\lambda = \lambda_a^{(1)} \phi,$$

$$\lambda_{tt\mu} = \lambda_{tt\mu}^{(1)} \phi. \tag{7}$$

In this notation $\phi = \rho/\rho_1$, is a relative target density referred to some arbitrarily chosen density ρ_1. The values of parameters quoted in the literature are usually referred to the density of liquid hydrogen ($\rho_1 = \rho_0 = 4.22 \cdot 10^{22} \text{cm}^{-3}$). For the purpose of this work it was more convenient, however, to let ρ_1 be chosen arbitrarily. In contrast to $\lambda_{tt\mu}$, the fusion rate λ_f and the sticking coefficient ω reflect intrinsic features of the nuclear interaction between tritons in the $tt\mu$ -molecule and do not depend on target characteristics.

According to the theoretical estimates the expected values of the parameters describing chain (4) are: $\lambda_a^{(0)} \approx 10^{11} \text{s}^{-1}$ /9/, $\lambda_{tt\mu}^{(0)} \approx 3 \cdot 10^6 \text{s}^{-1}$ /7/ , $\lambda_f = 10^6 \div 10^8 \text{s}^{-1}$ /8/ and $\omega = 0.05 \div 0.2$ /10/.

The set of Eqs.(6) can be solved in a routine way. However, the resulting expressions are quite lengthy and contain the physical parameters in a rather entangled form. The situation is considerably simplified if one takes into account that $\lambda_a^{(0)} \gg \lambda_0$. Then, for $\rho/\rho_0 \geq 10^{-2}$ and for $t_1 > \lambda_a^{-1}$ Eqs. (6.1) and (6.2) can be folded into one equation

$$\frac{dN_{t\mu}}{dt} = -(\lambda_0 + \lambda_{tt\mu}) N_{t\mu} + (1-\omega)\lambda_f N_{tt\mu}. \tag{6.5}$$

The characteristic equation for the set of Eqs. (6.3) and (6.5) gives the following expressions for the exponents of the partial solutions:

$$r_\pm = -\frac{1}{2} [2\lambda_0 + (\lambda_f + \lambda_{tt\mu})(1 \pm \sqrt{1-\kappa})], \tag{8}$$

where

$$\kappa = \frac{4\lambda_f \lambda_{tt\mu} \omega}{(\lambda_f + \lambda_{tt\mu})^2}. \tag{9}$$

Taking into account the initial conditions: $N_{tt\mu}(0) = 0$ and $N_{t\mu}(0) = 1$, one obtains the familiar form for the time distribution of the final neutrons per one muon stopped in the target:

$$\frac{dN_n}{dt} = 2B(e^{r_- t} - e^{r_+ t}), \tag{10}$$

where, for the experimentally observed time distribution,

$$B = \frac{\epsilon \lambda_f \lambda_{tt\mu}}{(\lambda_f + \lambda_{tt\mu}) \sqrt{1-\kappa}}, \tag{11}$$

ϵ being the registration efficiency of the $tt\mu$ -fusion events. Let us notice for further use that time distribution (10) has a maximun at

$$t_1 = \frac{\ln \left[\dfrac{2\lambda_0 + (\lambda_f + \lambda_{tt\mu})(1 + \sqrt{1-\kappa})}{2\lambda_0 + (\lambda_f + \lambda_{tt\mu})(1 - \sqrt{1-\kappa})} \right]}{(\lambda_f + \lambda_{tt\mu}) \sqrt{1-\kappa}} \tag{12}$$

and the total neutron yield corresponding to (10) is:

$$N_n^{(\infty)} = 2\epsilon \frac{\lambda_f \lambda_{tt\mu}}{\lambda_0^2 + \lambda_0(\lambda_f + \lambda_{tt\mu}) + \lambda_f \lambda_{tt\mu} \omega}. \tag{13}$$

To estimate the expected statistits and to enable one to determine the optimal conditions for the $tt\mu$ -fusion experiment (target density, time of switching-on neutron registration after the muon has stopped) it is useful to illustrate some of the above dependences. Fig.2 shows the total neutron yields calculated in the time interval $(0.025 \div 7.5)$ μs as a function of $\phi = \rho/\rho_1$ for several values of $\lambda_{tt\mu}^{(1)}$, λ_f and ω. Analogous plots for the slope of the long-time exponential, $S_{SLOW} = -r_-$, are shown in Fig.3. Fig.4 illustrates the dependence of t_1 on λ_f for a few values of $\lambda_{tt\mu}$ and ω. The content of these figures will be discussed in the next section.

In the limiting cases: $\lambda_f \gg \lambda_{tt\mu}$ and $\lambda_f \ll \lambda_{tt\mu}$, the total neutron yield $N_n^{(\infty)}$ exhibits the expected behaviour

$$N_n^{(\infty)} \longrightarrow 2\epsilon \frac{\lambda_s}{\lambda_0 + \lambda_s \omega} \xrightarrow{\lambda_0 \ll \lambda_s \omega} \epsilon \frac{2}{\omega}. \tag{14}$$

Additionally,

$$B \to \epsilon \lambda_s \tag{15}$$

and

$$t_1 \to \frac{1}{\lambda_\ell} \ln \left(\frac{\lambda_\ell + \lambda_0}{\lambda_0 + \omega \lambda_s} \right) \xrightarrow{\lambda_0 \ll \lambda_\ell} \frac{1}{\lambda_\ell} \ln \left(\frac{\lambda_\ell}{\lambda_0 + \omega \lambda_s} \right). \qquad (16)$$
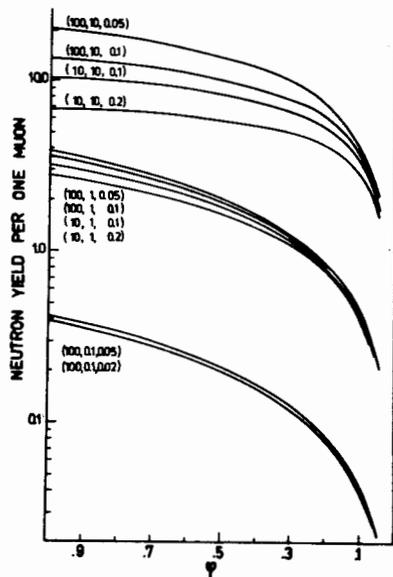
Fig.2. Total neutron yields in time interval 0-7.5 μs per one stopped muon vs target density for different values of $\lambda_{tt\mu}$, λ_f and ω. $\epsilon = 1$.
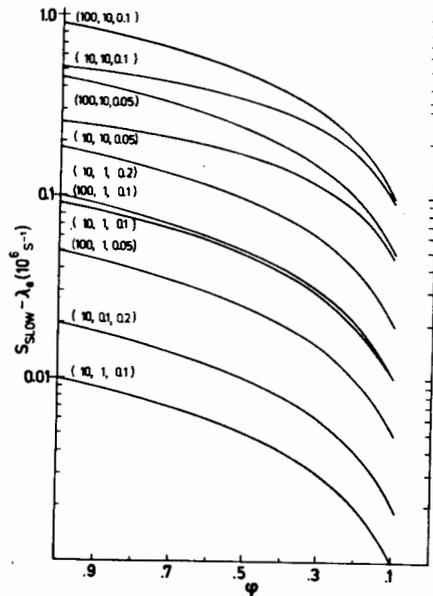
Fig.3. Difference between the slope of the long-time exponential in Eq. (10), S_{SLOW}, and the muon decay rate λ_0 vs target density for different values of $\lambda_{tt\mu}$, λ_f and ω.
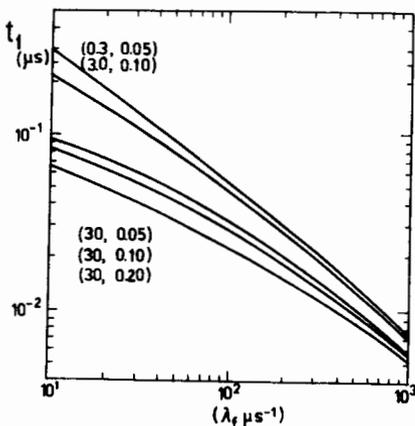
Fig.4. Position of the maximum, t_1 in the final neutron time distribution vs λ_f for several values of $\lambda_{tt\mu}$ and ω.

where $\lambda_s(\lambda_\ell)$ is the smaller (larger) of the two rates: λ_f and $\lambda_{tt\mu}$.

Let us also notice that since $\kappa \leq \omega$ and the expected value of ω is of the order of $\omega \approx 0.1$, the square-root in Eqs. (8), (11) and (12) can be expanded in terms of κ yielding, in particular, the following transparent expressions for the slopes of the exponential functions in the neutron time distribution (10)

$$S_{SLOW} = -r_- = \lambda_0 + \frac{\lambda_f \lambda_{tt\mu} \, \omega}{\lambda_f + \lambda_{tt\mu}} \xrightarrow{\lambda_s \ll \lambda_\ell} \lambda_0 + \omega \lambda_s \qquad (17a)$$

and

$$S_{FAST} = -r_+ = \lambda_0 + (\lambda_f + \lambda_{tt\mu}) - \frac{\lambda_f \lambda_{tt\mu} \, \omega}{\lambda_f + \lambda_{tt\mu}} \longrightarrow \lambda_0 + \lambda_\ell. \qquad (17b)$$

Below we analyse formulae (10)-(17) with the purpose of establishing the experimental conditions needed to determine the values of parameters λ_f, $\lambda_{tt\mu}$ and ω in an experiment with a pure tritium target. Of course, exactly the same formulae can be used to describe the kinetics of processes (3). However, as is mentioned earlier, the corresponding fusion rate in the $dd\mu$-molecule is very large as compared with the analogous rate for the $tt\mu$-molecule and simplified formulae taken at $\lambda_f^{(dd\mu)} \to \infty$ can be used. Thus, only two parameters, $\lambda_s = \lambda_{dd\mu}$ and ω_d, remain to be determined in the experiment with a pure deuterium target. The situation is different for channel (4) where λ_f and $\lambda_{tt\mu}$ may have similar values.

3. SENSITIVITY OF EXPERIMENTAL RESULTS TO THE VALUES OF PARAMETERS

A. Let us first make a trivial observation that formula (10) describing the final neutron time distribution is symmetric in λ_f and $\lambda_{tt\mu}$. Therefore, any fit of the data to Eqs. (10) or (13) will give two solutions corresponding to the transposition

$$(\lambda_f, \lambda_{tt\mu}) \leftrightarrow (\lambda_{tt\mu}, \lambda_f), \qquad (18)$$

which are indistinguishable on the basis of χ^2 alone. This ambiguity may become quite essential in the description of the full scheme of Fig.1, where $\lambda_{tt\mu}$ determines the fraction of muons entering the competitive channel leading to reaction (5). Of course, the data for a D_2-T_2 mixture combined with the data

for a pure T_2-target may enable one to resolve this ambiguity. However, regarding the compexity of the corresponding expressions, it is useful to have independent information about $\lambda_{tt\mu}$ and λ_f from the experiment with pure tritium.

Such information can be obtained if one takes into account relation (7) and constancy of λ_f with ϕ. The above-mentioned ambiguity is then avoided if the data for different target densities are analysed simultaneously.

To get a quantitative picture of how the situation may look like in an actual experiment the analysis of simulated results of a $tt\mu$-fusion experiment was performed for several values of $\lambda_{tt\mu}^{(1)}$, λ_f and ω. Time distributions (10) were constructed for $\phi_1 = 1$ and several values of $\phi_2 < 1$. Equal numbers of muons stopped in the target were assumed for both ϕ_1 and ϕ_2 which in accordance with Fig.2 gave smaller statistics at ϕ_2. The number of events in each time interval of the corresponding histograms was then randomly dispersed using the Poisson distribution. The time distributions obtained in this way were subsequently fitted with formula (10) using two different sets of the starting parameter values:

i) the values close to those used initially in the construction of the histograms (input solution) and

ii) the same values with λ_f and $\lambda_{tt\mu}^{(1)}$ interchanged (inverse solution).

The minumum in χ^2 corresponding to the inverse solution has been found to survive up to quite high values of

$$a_1 = \frac{\lambda_f}{\lambda_{tt\mu}^{(1)}} \tag{19}$$

($a_1 \approx 15$), which indicates that in the analysis of future data any such minimum should be checked against the solution with λ_f and $\lambda_{tt\mu}^{(1)}$ interchanged. Figure 5 shows the difference between the χ^2-value for the inverse solution and the corresponding value for the input solution as a function of a_1, for several values of $\lambda_{tt\mu}^{(1)}$ and $\omega = 0.1$. It is seen that even with moderate statistics ($N_n \approx 2 \cdot 10^5$ neutrons) and ϕ_2 quite close to $\phi_1 = 1$ ($\phi_2 \approx 0.9$) the two solutions can be distinguished at about 90% confidence level for $a_1 \geq 2.0$ and $a_1 \leq 0.5$ and, practically, for any $\lambda_{tt\mu}^{(1)}$. The situation can be further improved by increasing the statistics or decreasing ϕ_2 which is also illustrated in the figure. Similar behaviour of $\chi_{INV}^2 - \chi_{INP}^2$ with a_1 has been found for $\omega = 0.05$ and 0.2.

It is interesting to observe that the temperature variation of the density of liquid tritium (deuterium) in a rather small range above the temperature of liquid hydrogen (20.4K) is sufficient to cover such changes of ϕ (see Fig.9). This, in particular, enables one to determine the $tt\mu$-fusion parameters in the experiment with a liquid tritium target.
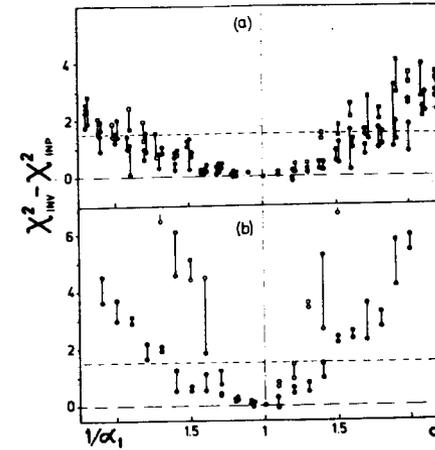
Fig.5. Difference between the χ^2-values corresponding to inverse and input solutions obtained in the fits of the simulated data to formula (10) as a function of $a_1 = \lambda_f / \lambda_{tt\mu}^{(1)}$ (the right-hand part of the horizontal scale) and a_1^{-1} (the left-hand part). The upper section corresponds to ($\phi_1 = 1$, $\phi_2 = 0.9$) and the lower one to ($\phi_1 = 1$, $\phi_2 = 0.85$). Full circles correspond to $\lambda_{tt\mu}^{(1)} = 1 \ \mu s^{-1}$, crossed circles to $20 \ \mu s^{-1}$ and rectangles to $100 \ \mu s^{-1}$ and to statistics of $2 \cdot 10^5$ neutrons. Open circles in the lower section correspond to $\lambda_{tt\mu}^{(1)} = 1.0 \ \mu s^{-1}$ and increased statistics (10^6 neutrons). Vertical lines connect points obtained in two different simulations. Dashed horizontal lines indicate $\chi^2 = 1.5$, χ^2 is in units of $\sqrt{2n_D}$ with the number of degrees of freedom $n_D \approx 600$ in the fits.

Let us also remark without going into details that, if the theoretical values of $\lambda_{tt\mu}^{(0)}$ and λ_f are not grossly overestimated and ϵ is of the order of 10%[*] the required statistics (according to Fig.5, about 10^5 registered fusion events) can be easily obtained within a few hours, especially in the experiment with a liquid tritium target. Thus, contamination of tritium in the target by ^3He produced in tritium β-decay can be kept below $c_{3_{He}} \approx 10^{-5}$. Such concentrations of ^3He lead to negligibly small rates of the mesomolecular processes involving ^3He as compared with the analogous rates for T_2. This justifies the assumption made in writing-down the kinetic equations (6).

B. Once for the reason described above ϕ has to be changed, it is interesting to see what is the effect of varying target density on the accuracy of determination of the $tt\mu$-fusion parameters. Let us limit ourselves to the case where measurements are performed at two densities: $\phi_1 = 1$ and $\phi_2 < 1$.

Increase in the separation between ϕ_1 and ϕ_2 will obviously tend to give better resolution between the two sets of data. However, such effect will be partly reduced by several factors:

---

[*] The value of registration efficiency obtained in Ref./11/ for the $tt\mu$-fusion experiment with a liquid tritium target is of this order of magnitude.

i) decreasing statistics (see Fig.2);

ii) decreasing sensitivity of the experimental characteristics to the values of parameters (see Figs.2 and 3);

iii) increasing correlations between the sought-for parameters. (As is shown below, these correlations become increasingly significant with growing $a = \lambda_f / \lambda_{tt\mu} \sim \phi^{-1}$, for $\lambda_f > \lambda_{tt\mu}^{(1)}$).

Consider first the possibility of $\lambda_f \approx \lambda_{tt\mu}^{(1)}$. In this case it is convenient to use the following independent combinations of the parameters entering Eq. (10):

$$P = S_{SLOW} + S_{FAST} - 2\lambda_0 = \lambda_f + \phi \lambda_{tt\mu}^{(1)} , \qquad (20a)$$

$$Q = B (S_{FAST} - S_{SLOW}) = \epsilon \lambda_f \lambda_{tt\mu}^{(1)} \phi , \qquad (20b)$$

$$R = \phi (S_{SLOW} - \lambda_0)^{-1} \approx \frac{1}{\lambda_{tt\mu}^{(1)} \omega} + \frac{1}{\lambda_f \omega} \phi . \qquad (20c)$$

Let us assume first that the contribution of the short-time exponential, $\exp(-S_{FAST}t)$, to the neutron time distribution (10) is seen in the data, i.e., the minimum time t_0 at which the neutron time distribution is measured is

$$t_0 \leq t_1 . \qquad (21)$$

Then, Eqs. (20) show that the data for two different values of ϕ allow a two-constraint determination of all parameters, including the registration efficiency ϵ. If the short-time exponential is not observed, information contained in parameter S_{FAST} is lost. However, a no-constraint determination of all parameters including ϵ is still possible which is best seen if one takes parameter R defined in Eq. (20c) and parameter

$$\bar{B} = B^{-2}\phi^2 = \frac{\phi^2}{(\epsilon\lambda_f)^2} + \frac{2(1-2\omega)\phi}{(\epsilon\lambda_f)(\epsilon\lambda_{tt\mu}^{(1)})} + \frac{1}{(\epsilon\lambda_{tt\mu}^{(1)})^2} . \qquad (22)$$

The situation is different for $\lambda_f \gg \lambda_{tt\mu}^{(1)}$ or $\lambda_f \ll \lambda_{tt\mu}^{(1)}$. Let us consider only the first case as the second one is rather unlikely. A convenient choice of the independent combinations of parameters is here:

$$\bar{P} = S_{FAST} - \lambda_0 \approx \lambda_f (1 + \frac{1-\omega}{a}) \qquad (23a)$$

$$\bar{Q} = B \approx \epsilon \lambda_{tt\mu}^{(1)} \phi (1 - \frac{1-2\omega}{a}) \qquad (23b)$$

$$\bar{R} = S_{SLOW} - \lambda_0 \approx \omega \lambda_{tt\mu}^{(1)} \phi (1 - \frac{1}{a}) , \qquad (23c)$$

where $a = a_1 / \phi \sim \phi^{-1}$.

At large a Eqs. (23b) and (23c) decouple from Eq. (23a). Parameters $\lambda_{tt\mu}^{(1)}$ and ω can be now determined from the slope of dN_n/dt at large t and the value of the preexponential factor B, provided the registration efficiency ϵ is known.

Let us remark that in the limiting case, $a \to \infty$, information contained in the data for different densities is not independent, and measuring dN_n / dt at one density would be sufficient for the determination of λ_f, $\lambda_{tt\mu}$ and ω. Still, resolving the $\lambda_f \leftrightarrow \lambda_{tt\mu}$ ambiguity requires the data at two values of ϕ.

Let us also notice that, as seen from Eqs. (23), parameters ϵ, ω and $\lambda_{tt\mu}^{(1)}$ become strongly correlated* as $a \to \infty$. In this limiting case the possible solutions of χ^2-minimization can be expected to lie on the one-dimensional trajectory:

$$\lambda_{tt\mu}^{(1)} (\epsilon) = \frac{\bar{Q}}{\epsilon} , \qquad \omega(\epsilon) = \frac{\bar{R}}{\bar{Q}} \epsilon . \qquad (24)$$

Therefore, if a is large one will, probably, have to determine ϵ independently in order to be able to find the remaining parameters from the data. Of course, for finite a the corrections in the brackets on the RHS of Eqs. (23) bring one, in principle, back to the situation considered above for $\lambda_f \approx \lambda_{tt\mu}^{(1)}$ where ϵ can be extracted from the measured neutron time distribution together with the other parameters. However, if the corrections themselves are comparable with the experimental uncertainties, achieving reasonable accuracy using such a procedure becomes questionable. To illustrate this point Fig.6 shows the difference between the χ^2-value at some point on trajectory (24) and the χ^2-value of the best fit corresponding to the input solution ($\lambda_f = 50$ μs^{-1}, $\lambda_{tt\mu}^{(1)} = 3$ μs^{-1}, $\omega = 0.1$, $\epsilon = 1$) as a function of ϕ_2 ($\phi_1 = 1$). Different curves which are hand drawn to guide the eye correspond to $\epsilon = 0.75$, 0.67 and 0.5. It is seen that even for the values of parameters deviating by ~30% from the input values it is practically impossible to distinguish the solutions along the trajectory on the basis of χ^2 if ϵ is left free in the fits. Therefore, achieving better accuracy in the experiment will require independent constraining of ϵ. The situation improves with decreasing a_1 and, according to our estimates, for $a_1 \lesssim 4.0$ there may exist

---

* In fact, in the simulation of the $tt\mu$-data described above, the correlation coefficients estimated by subroutine Hesse after the Simplex minimization [12] were practically: $C(\epsilon, \lambda_{tt\mu}^{(1)}) = -1$, $C(\lambda_{tt\mu}^{(1)}, \omega) = -1$ and $C(\epsilon, \omega) = +1$, already for $a \gtrsim 3 \div 5$.
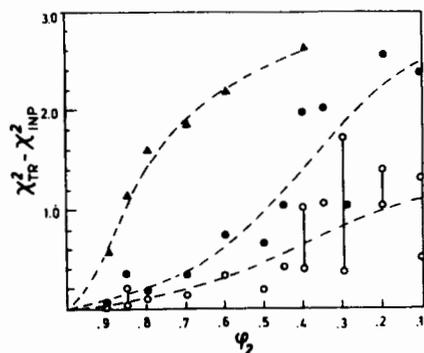
Fig.6. Difference between χ^2 corresponding to solutions on trajectory (24) and χ^2 of the input solution for $\lambda_f = 50~\mu s^{-1}$, $\lambda_{tt\mu}^{(1)} = 3~\mu s^{-1}$, $\omega = 01$ and $\epsilon = 1$, vs ϕ_2 ($\phi_1 = 1$). Open and closed circles and triangles correspond to $\epsilon = 0.75$, 0.67 and 0.5, respectively. Curves are hand-drawn to guide the eye. χ^2 defined as in Fig.5. Statistics: 10^6 neutrons for ϕ_1.
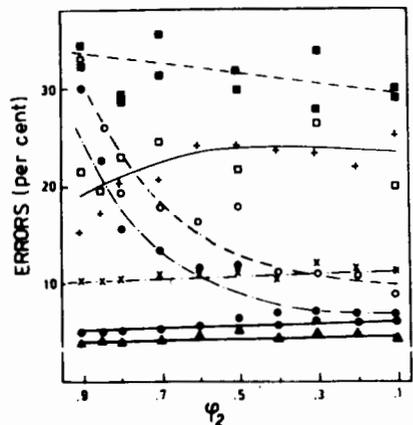
Fig.7. Simplex estimates of errors corresponding to input solutions vs ϕ_2 ($\phi_1 = 1$). Statistics is 10^6 neutrons for ϕ_1. O, $\oplus$, $\bullet$, and $\blacktriangle$ represent $\Delta\lambda_f/\lambda_f$, $\Delta\lambda_{tt\mu}^{(1)}/\lambda_{tt\mu}^{(1)}$, $\Delta\omega/\omega$ and $\Delta\epsilon/\epsilon$, respectively, for $\lambda_f = \lambda_{tt\mu}^{(1)} = 10\mu s^{-1}$, $\omega = 0.1$, $\epsilon = 1$. Analogously, $\square$, $\boxminus$ and $\blacksquare$ are for $\lambda_f = 30~\mu s^{-1}$, $\lambda_{tt\mu}^{(1)} = 10~\mu s^{-1}$ ($\Delta\omega/\omega$ and $\Delta\epsilon/\epsilon$ coincide). Bare crosses $\times$ and $+$ represent $\Delta\lambda_f/\lambda_f$ and $\Delta\lambda_{tt\mu}^{(1)}/\lambda_{tt\mu}^{(1)}$ $\simeq \Delta\omega/\omega \simeq \Delta\epsilon/\epsilon$ for $\lambda_f = 50~\mu s^{-1}$

and $\lambda_{tt\mu}^{(1)} = 3~\mu s^{-1}$, respectively. Curves are hand-drawn to guide the eye.

a possibility of determining ϵ from the data at the level of $\Delta\epsilon/\epsilon \approx 10\%$, even if ϕ_2 is chosen in the region: $\phi_2 = 0.8-0.6$. However, for $a_1 \geq 4.0$ an independent determination of the registration efficiency will be perhaps necessary.

To illustrate the interplay of different factors (i-iii), the Simplex[12] estimates to errors obtained in the fits of the simulated data are shown in Fig.7 as a function of ϕ_2. It is seen that increase in the separation between ϕ_1 and ϕ_2 brings only a limited advantage. For $\lambda_f \approx \lambda_{tt\mu}^{(1)}$ the accuracy of the determination of these two parameters increases, which is obvious from the linear dependence of Eq. (20a), while the corresponding errors of ω and ϵ are constant or even slightly increasing. Starting from $a_1 \approx 3$ no effect of varying ϕ_2 is clearly noticeable. The figure suggests that the optimum choice of ϕ_2 is in the region of $\phi_2 = 0.5-0.4$.

(a) $\lambda_f (\mu s^{-1})$ (b)
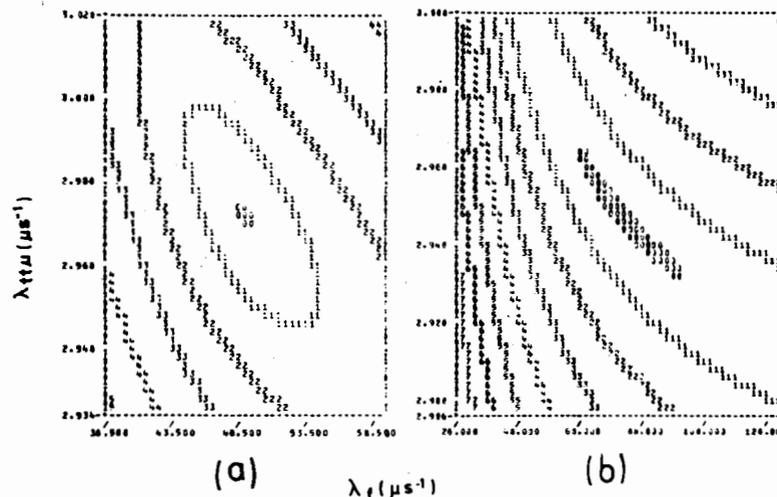
Fig.8. Contour plots of equal χ^2 in (λ_f, $\lambda_{tt\mu}^{(1)}$)-plane for different t_0-cuts: $0.025~\mu s$ and $0.125~\mu s$ (sections a and b, respectively). The minimum corresponds to input solution: $\lambda_f = 50~\mu s^{-1}$, $\lambda_{tt\mu}^{(1)} = 3~\mu s^{-1}$, $\omega = 0.1$, for which $t_1 = 0.080~\mu s$. The innermost contour (1) corresponds to $\chi_{min}^2 + 1$. Statistics: 10^6 neutrons for $\phi_1 = 1$ ($\phi_2 = 0.85$).
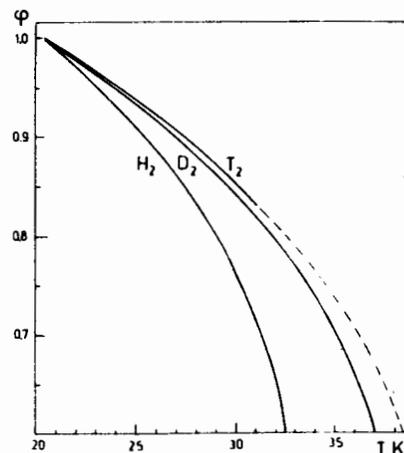
Fig.9. Density variation of liquid hydrogen, deuterium and tritium with temperature. Ordinate is relative density referred to the density of liquid hydrogen at 20.4K. Solid curves represent measured values[13] the dashed ones are extrapolations.

Finally, let us briefly discuss the influence of the t_0-cut in the neutron time distribution on the accuracy of the determination of λ_f. Figs.(8a-b) show the χ^2-contours in the (λ_f, $\lambda_{tt\mu}^{(1)}$)-plane for the simulated data obtained with (λ_f, $\lambda_{tt\mu}^{(1)}$, ω)=

= (50 μs^{-1} ; 3 μs^{-1} , 0.1). Different sections correspond to t_0 = 0.025 μs, and 0.125 μs, respectively. It is seen that the accuracy of the determination of λ_f decreases rapidly with increasing t_0, so that for t_0 above t_1 (t_1 = 0.08 μs in this case), practically only a lower limit can be set on λ_f. Confronting the patterns of Fig.8 with the curves shown in Fig.4 one can see that choosing $t_0 \approx 0.01$ μs should secure the possibility of determining λ_f with reasonable accuracy, if the existing theoretical predictions are not grossly underestimated. This indicates that there is a realistic possibility of confronting the model calculations of λ_f for $tt\mu$-fusion with experimental data which, in practice, does not exist for reactions (1) and (2). The existence of such a possibility should justify the effort of choosing $t_0 \leq 0.01$ μs.

4. CONCLUSIONS

As has been shown in the previous section, measuring the neutron time distributions at two target densities in both necessary and sufficient to assign unambiguously the experimental values to the parameters characterizing the $tt\mu$-fusion in the experiment with a pure tritium target. The choice of two densities which differ by about 20% should enable one to differentiate between the $tt\mu$-molecule formation rate $\lambda_{tt\mu}$ and the corresponding fusion rate λ_f if $\lambda_f/\lambda_{tt\mu} \geq 2$ or $\lambda_f/\lambda_{tt\mu} \leq 0.5$, even with quite moderate statistics. Such variation of the density falls within the range of density variation of liquid tritium with temperature in a rather small interval above the temperature of liquid hydrogen (20.4K). This, in particular, renders feasible the determination of $tt\mu$-formation rate at a very low temperature, which can provide an important piece of information for establishing the behaviour of $\lambda_{tt\mu}$ with collision energy. Apart from the increased statistics which can be secured with a high-density target and the technical advantages of working with liquid tritium (connected with severe safety requirements), sensitivity of the results to the values of parameters in such experiment is higher than in the experiment with a gaseous target where practically achievable densities are significantly lower.

If one decides to verify the theoretical prediction of absence of the temperature dependence of $\lambda_{tt\mu}$, data have to be taken at substantially higher temperatures, i.e., in the experiment with a gaseous target. Assuming that the temperature - independent parameters, ω and λ_f, are determined in a liquid target experiment, it is enough to measure the neutron time distribution at one density (desirably as high as possible). Nevertheless, regarding the facility with which density can be changed in this case, it may become temping to get a full picture at another temperature. According to the arguments presented in the previous section, the choice of densities which differ by a factor of ~0.4÷0.5 should be optimal in this case.

REFERENCES

1. Fetkovich J. et al. Phys.Rev.Lett., 1960, 4, p.570; Doede J. et al. Phys.Rev., 1963, 132, p.1732; Dzhelepov V.P. et al. Zh.Eksp.Theor.Fiz., 1966, 50, p.1235; Zmeskal J. et al.In: Proc. of the Third Int.Conf.On Emerging Nucl.Systems. Helsinki, June, 1983.
2. Bystritsky V.M. et al. Zh.Eksp.Theor.Fiz., 1979, 76, p.460.
3. Bystritsky V.M. et al. Zh.Eksp.Theor.Fiz., 1981, 80,p.1700; Jones E. et al. In: Proc. of the Third Int.Conf.on Emerging Nucl. Systems, Helsinki, June 1983.
4. Vesman E.A. Pisma Zh.Eksp.Theor.Fiz., 1967, 5, p.113; Gerstein S.S., Ponomarev L.I. Phys.Lett., 1977, 72B, p.80; Vinitsky S.I. et al. Zh.Eksp.Theor.Fiz., 1978, 74, p.839.
5. Petrov Yu.V. Nature, 1980, 285, p.466; Ponomarev L.I. JINR, P4-81-800, Dubna, 1981.
6. Balin O.V., Vorobev A.A. et al. In: Proc. of the Third Int. Conf.on Emerging Nuclear Systems. Helsinki, June 1983.
7. Ponomarev L.I., Faifman M.P. Zh.Eksp.Theor.Fiz., 1976,71, p.1689.
8. Melezhik V.S. JINR, 4-81-463, Dubna, 1981.
9. Korenman G.Ya. Yad.Fiz., 1980, 32, p.916; Markushin V.E. Zh.Eksp.Theor.Fiz., 1981, 80, p.35; Cohen J.S., Martin R.L., Wadt W.R. Phys.Rev., 1981, 24A, p.33.
10. Gerstein S.S. et al. Zh.Eksp.Theor.Fiz., 1981, 80, p.1690.
11. Bystritsky V.M. et al. JINR, P1-83-515, Dubna, 1983.
12. James F., Ross M. Minuit. CERN Long Write-Up, 1971.
13. Malkov M.P. et al. Spravochnik po fiziko-tekhnicheskim osnovam kriogeniki, Energia, Moscow, 1973.

Быстрицкий В.М. и др.   E1-83-690

Определение оптимальных условий экспериментов
по исследованию мюонного катализа
ядерной реакции $t + t \rightarrow {}^4He + 2n$

В работе проводится анализ формул, описывающих кинематику процесса мюонного катализа ядерной реакции синтеза $t + t \rightarrow$ $\rightarrow {}^4He + 2n$ в чистом тритии, с целью определения оптимальных условий проведения экспериментов по измерению параметров данного процесса. Показано, что для определения таких параметров необходимо выполнение измерений при различной плотности мишени. Определен требуемый диапазон изменения плотности мишени, исходя из теоретически предсказанных значений параметров процесса μ-катализа в чистом тритии. В частности, показано, что требуемый диапазон изменения плотности трития достигается при небольшом повышении температуры относительно температуры жидкого водорода /20,4°К/.

Работа выполнена в Лаборатории ядерных проблем ОИЯИ.

Bystritsky V.M. et al.   E1-83-690
Determination of Optimal Conditions
for the Experimental Investigation of Muon Catalysis
of Nuclear Reaction: $t + t \rightarrow {}^4He + 2n$

Formulae describing the kinetics of muon-catalysed fusion $t + t \rightarrow {}^4He + 2n$ in pure tritium are analysed with the aim of establishing optimum conditions for the experimental investigation of $tt\mu$-fusion. It is shown that to determine the parameters characterizing $tt\mu$-fusion in an experiment with a pure tritium target data have to be taken at different target densities. The range of variation of target density, required to cover the region of parameter values predicted theoretically, is determined. In particular, it is shown that temperature variation of the density of liquid tritium in a rather small range above the temperature of liquid hydrogen (20.4K) is sufficient in this kind of experiment.

The investigation has been performed at the Laboratory of Nuclear Physics, JINR.